

The Journal of Strain Analysis for Engineering Design

<http://sdj.sagepub.com/>

Investigation of the dependences of the mechanical characteristics of an alloyed steel on both the strain rate and the microstructure

M Homayonifar, M Zebarjad, A Sajjadi and A Saatian

The Journal of Strain Analysis for Engineering Design 2007 42: 105

DOI: 10.1243/03093247JSA202

The online version of this article can be found at:

<http://sdj.sagepub.com/content/42/2/105>

Published by:



<http://www.sagepublications.com>

On behalf of:



[Institution of Mechanical Engineers](http://www.imeche.org)

Additional services and information for *The Journal of Strain Analysis for Engineering Design* can be found at:

Email Alerts: <http://sdj.sagepub.com/cgi/alerts>

Subscriptions: <http://sdj.sagepub.com/subscriptions>

Reprints: <http://www.sagepub.com/journalsReprints.nav>

Permissions: <http://www.sagepub.com/journalsPermissions.nav>

Citations: <http://sdj.sagepub.com/content/42/2/105.refs.html>

>> [Version of Record](#) - Jan 1, 2007

[What is This?](#)

Investigation of the dependences of the mechanical characteristics of an alloyed steel on both the strain rate and the microstructure

M Homayonifar, M Zebarjad*, A Sajjadi, and A Saatian

Department of Material Science and Engineering, Engineering Faculty, Ferdowsi University, Mashhad, Iran

The manuscript was received on 7 January 2006 and was accepted after revision for publication on 23 August 2006.

DOI: 10.1243/03093247JSA202

Abstract: The mechanical properties of AISI 4140 steel were studied at different strain rates (0.167, 0.833, and 1.667 min⁻¹) for various microstructures. To investigate the influence of microstructure, spheroidizing, normalizing, and quench tempering (single tempered and double tempered) were used to obtain a range of microstructures and strength levels. To study the dependences of the mechanical characteristics of AISI 4140 steel on both the strain rate and the microstructure, tensile tests and microscopic evaluation were performed.

The results showed that not only do the yield and the ultimate strength depend on both the microstructure and the strain rate but also so does the appearance of the yielding phenomenon. Also the results showed that an increase in strain rate causes the strain-hardening exponent n and the strength coefficient K to decrease in both quench-tempered and normalized structures but has a negative effect on the spheroidized structure. In fact, the sensitivity of the spheroidized structure to the strain rate is higher than those of the other structures. Microscopic evaluation proved that the Lüders strain width of the spheroidized microstructure is much lower, because of its soft ferrite matrix.

Keywords: alloyed steel, strain rate, microstructure, mechanical characteristics, Lüders strain, yielding phenomenon

1 INTRODUCTION

One of the most utilizable medium-carbon ultrahigh-strength steels in the automotive industries is AISI 4140 because of its moderate hardenability, good strength, and toughness. Although the alloy can be used in many applications, its applications have been limited relative to its potential. With regards to the vast applications, many researchers are interested in investigating the steel in more detail. According to a literature survey, their studies can be divided into five approaches [1–26]. The first approach concentrated on the role of austenite grains in the mechanical properties of AISI 4140. In fact, investigators believed that the steel in the quenched-and-tempered condition possesses a fine dispersion of ferrite–cementite mixture which caused a relatively good ratio of yield

strength to toughness. In this condition the grain refining of primary austenite grains makes the steel tougher and stronger [2–5]. The second approach paid attention to the dependences of the mechanical properties of AISI 4140 on conventional heat treatment and cyclic heat treatment [6–10]. The results showed that the mechanical properties depend strictly on the heat treatment. In fact, some properties are enhanced and others are reduced as a result of heat treatment. Smoljan [6] applied an appropriate cyclic heat treatment and showed that the yield stress and toughness improved with respect to the results from a conventional quenched-and-tempered treatment. The third approach focused on the elastic properties of AISI 4140 [11–13]. Determination of the shear and Young's modulus by using ultrasound spectroscopy, impulse excitation, nanoindentation, and destructive methods were carried out by those investigators. The fourth approach tried to predict the mechanical properties of AISI 4140 by using specific equations particularly at higher temperatures and various

* Corresponding author: Department of Material Science and Engineering, Engineering Faculty, Ferdowsi University, PO Box 91775-1111, Mashhad, Iran. email: zebarjad@ferdowsi.um.ac.ir

strain rates [14–18]. The presented models give the flow stress of carbon steels as a function of the strain, strain rate, temperature, and carbon content. The fifth approach considered the relationship between the residual stresses due to heat treatment and the tensile properties of AISI 4140 [19–23]. The results show that the yield stress and ultimate stress can be affected by the residual stress. Also it has been proved that the magnitude of the residual stress depends strongly on the kind of heat treatment. For example the effect of normalizing is greater than the effect of quench tempering [19].

From the literature review performed by the present authors, it was found that many researchers [1–26] have studied the effect of normalizing, annealing, and quench-tempering heat treatments on the mechanical properties such as the hardness, yield stress, and tensile stress but there is no evidence of the investigation of the effects of both heat treatment and strain rate on mechanical characteristics such as the strain-hardening exponent n , strength coefficient K , and strain rate sensitivity m . Also the roles of both the heat treatment and the strain rate in the yielding phenomenon has not attracted attention. Therefore, the main goal of the current study is to elucidate the effect of normalizing, spheroidizing, and quench-tempering heat treatments and strain

rate on the mechanical characteristics of AISI 4140 steel. Also attempts were made to clarify the yielding phenomenon mechanism.

2 EXPERIMENTAL PROCEDURE

2.1 Materials

AISI 4140 steel was obtained from Yazd Alloying Steel Complex (Iran-Yazd). The chemical composition of the used material is summarized in Table 1.

2.2 Heat treatment

Different heat treatment cycles were applied to 12 AISI 4140 steel billets of 20 mm diameter and 100 mm length. To eliminate the history of the alloys, all samples were annealed at 815 °C for 20 min. Then the specimens were cooled to room temperature in glass wool to achieve a cooling rate of about 1–2 °C/min [3]. Details of the heat treatment cycles applied to the specimens are summarized in Table 2.

The spheroidizing heat treatment was applied to the first three specimens (specimens 1, 2, and 3). The specimens were heated to 750 °C and held in the furnace for 7 h. Specimens 4, 5, and 6 were

Table 1 Chemical composition of AISI 4140 steel

Element	C	Mn	Si	Cr	Mo	S	P
Amount (wt %)	0.42	0.8	0.4	1.1	0.25	0.03	0.035

Table 2 Heat treatment cycles for the specimens

Specimen	Spheroidizing temperature (°C)	Spheroidizing time (h)	Cooling condition				
1	750	7	Furnace cooled				
2	750	7	Furnace cooled				
3	750	7	Furnace cooled				
Specimen	Normalizing temperature (°C)	Normalizing time (min)	Cooling condition				
4	870	30	Stilled air				
5	870	30	Stilled air				
6	870	30	Stilled air				
Specimen	Austenitizing temperature (°C)	Austenitizing time (min)	Quench medium	First tempering temperature (°C)	First tempering time (min)	Second tempering temperature (°C)	Second tempering time (min)
7	855	30	Turbulent oil	620	120	–	–
8	855	30	Turbulent oil	620	120	–	–
9	855	30	Turbulent oil	620	120	–	–
10	855	30	Turbulent oil	430	60	–	–
11	855	30	Turbulent oil	180	60	350	60
12	855	30	Turbulent oil	230	30	230	30

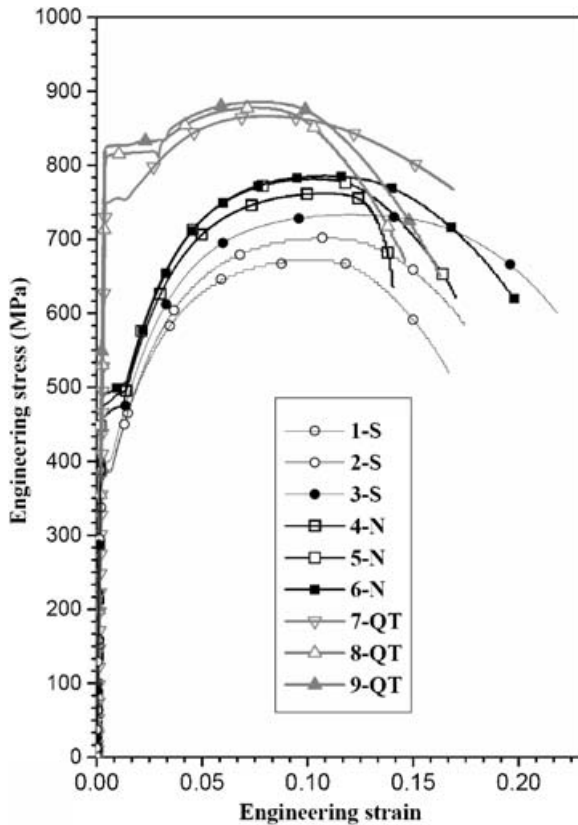


Fig. 2 Engineering stress–engineering strain curves for specimens 1 to 9 as a function of strain rate. N, QT, and S indicate normalized, quench-tempered, and spheroidized samples respectively

Table 4 Mechanical properties of specimens 1 to 9

Specimen	Strain rate (min^{-1})	Yield stress (MPa)	Tensile stress (MPa)
<i>Spheroidized</i>			
1	0.167	381.48	671.28
2	0.833	388.12	702.33
3	1.667	395.55	732.72
<i>Normalized</i>			
4	0.167	460.26	761.97
5	0.833	476.64	781.55
6	1.667	491.59	785.57
<i>Quench tempered</i>			
7	0.167	749.07	866.33
8	0.833	812.98	877.69
9	1.667	825.63	885.46

increasing the strain rate has more effect on the ultimate tensile stresses of spheroidized specimens. So, changing the strain rate from 0.167 to 1.667 min^{-1} causes an increase about 61.44 MPa in the ultimate tensile stress. This increase is only about 19.13 MPa for quench-tempered specimens. In the case of normalized specimens, decoupling the strain rate increases the yield stress by about 31.33 MPa and the ultimate tensile stress by about 23.6 MPa.

Also Fig. 2 shows that AISI 4140 steel has a considerable yield point phenomenon because of its chemical composition. Although the major reason for the yield point in AISI 4140 steel is the presence of interstitial carbon and nitrogen which, under appropriate conditions, lock the dislocations, the presence of manganese, silicon, chromium, molybdenum, sulphur and phosphorus cannot be ignored. For example, molybdenum behaves like a carbide former (Mo_2C); thus it can suppress the yielding point. However, according to what has been proposed by other investigators [28–30] the additions of 0.3–2 wt%Mo has a little effect on the yield point and silicon acting alone cannot eliminate the yield point phenomenon particularly for low silicon additions (less than 25 wt%). The effect of silicon, acting in conjunction with aluminium is very interesting. Silicon forms a stable nitride (SiN) and can be isomorphous with AlN . Both SiN and AlN precipitate and reduce the role of nitrogen in the yield point.

With regard to Fig. 2 it can be seen that different heat treatment cycles change the behaviour of this phenomenon. The reason for this variation can be explained easily as follows. On quenching to room temperature, the solute atoms are frozen in a random distribution through the matrix, the dislocations are free of solute atmospheres, and the initial yield point is not present. However, after tempering the supersaturated lattice, much of the excess solute will be precipitated, and the dislocations will again become locked, so that the yield point will appear. On the other hand, the act of quench tempering or even furnace cooling will in general produce dispersion precipitates which will ensure that a large fraction of the dislocations are locked in position by precipitates. This is why the yielding phenomenon can appear after the quench-tempered treatment. The results show that spheroidizing can decrease the Lüders strain and an increase in strain rate causes this strain to increase [31, 32]. The reason for this variation can be attributed to the fact that the Lüders extension depends on the microstructure and work-hardening exponent; since the yield point phenomenon depends on the stiffness of the material, thus the yield point and the Lüders strain will be masked as the temper temperature decreases (see Fig. 2 and also Fig. 7 later) [31].

Figure 3 shows the true stress–true strain curves in the work-hardening stage (before necking), for specimens 1 to 9. The engineering stress and strain were changed to the true stress and strain using [33]

$$\varepsilon = \ln(1 + e) \quad (1)$$

$$\sigma = s(1 + e) \quad (2)$$

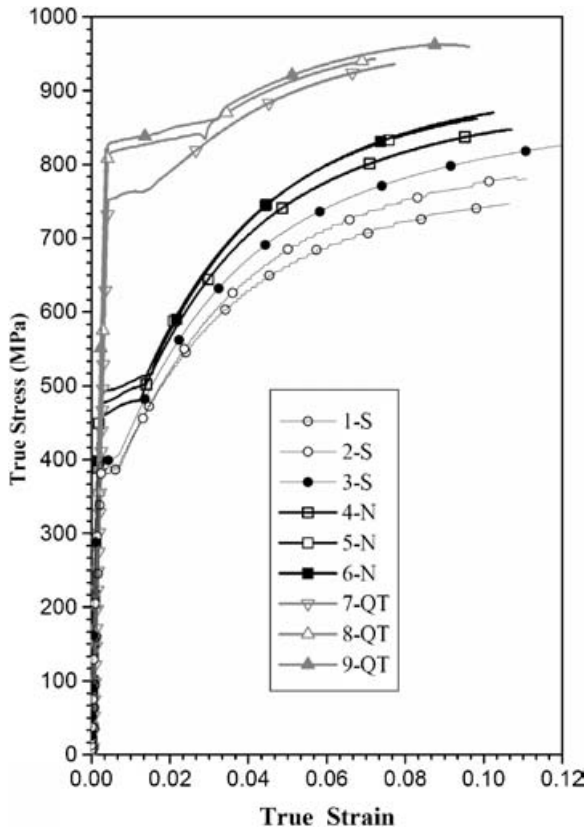


Fig. 3 True stress–true strain curves of specimens 1 to 9 before necking at different strain rate (0.167, 0.833 and 1.667 min⁻¹). N, QT, and S indicate normalized, quench–tempered, and spheroidized samples respectively

where e , s , ϵ , and σ are the engineering strain, the engineering stress, the true strain, and the true stress, respectively.

There are some equations that can estimate the relation between the stresses and strains in the work-hardening stage of stress–strain curves. However, the homogenous deformation part of stress–strain curves of many metals and steels can be explained by a simple power law consisting of the strength coefficient K and the strain-hardening exponent n according to

$$\sigma = K\epsilon^n \tag{3}$$

The parameters of the power law, namely n and K , can be found from log–log true stress–true strain curves. In these curves the strain-hardening factor n is the slope of these lines and the magnitude of $\log(\sigma)$ for $\epsilon = 1$ equals $\log(K)$, as given by

$$\log(\sigma) = \log(K) + n \log(\epsilon) \tag{4}$$

Figure 4 shows on a log–log scale the homogenous deformation part of the true stress–true strain curves of specimens 1 to 9. It can be seen that all curves

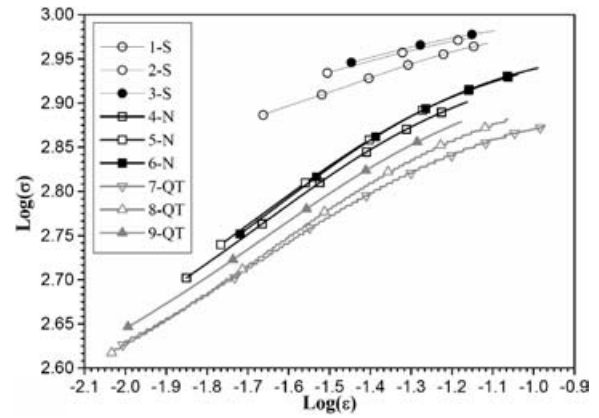


Fig. 4 Work-hardening part of true stress–true strain curves for specimens 1 to 9 on a logarithmic scale. N, QT, and S indicate normalized, quench–tempered, and spheroidized samples respectively

approximately follow linear behavior at lower strains and are deflected near the strain corresponding to the ultimate tensile stress; however generally they can be estimated from a linear equation [equation (4)]. The parameters which are determined from Fig. 4 are shown in Fig. 5 as functions of the strain rate. With

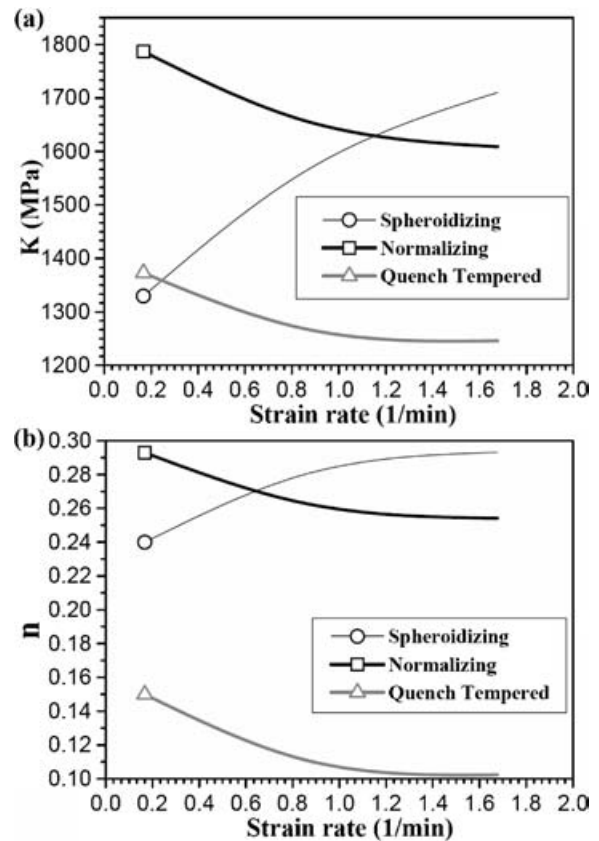


Fig. 5 Dependences of the mechanical characteristics of AISI 4140 steel on the strain rate after different heat treatments: (a) K ; (b) n

regard to Fig. 5 it can be concluded that the work-hardening exponent n depends on the microstructure. In fact, the higher value of n in the spheroidized microstructure can be attributed to coarse carbide particles which are surrounded by a soft ferrite matrix.

The flow stress in the homogenous deformation part of the stress–strain curves can also be estimated by another equation which relates the flow stress to the strain rate [33] according to

$$\sigma = C(\dot{\epsilon})^m \tag{5}$$

where

$$m = \frac{\left\{ \frac{\partial[\log(\sigma)]}{\partial[\log(\dot{\epsilon})]} \right\}_{\epsilon,T}}{\left\{ \frac{\Delta[\log(\sigma)]}{\Delta[\log(\dot{\epsilon})]} \right\}_{\epsilon,T}} \approx \frac{\log(\sigma_2) - \log(\sigma_1)}{\log(\dot{\epsilon}_2) - \log(\dot{\epsilon}_1)} \tag{6}$$

where m is the strain rate sensitivity parameter and C is a constant value. The results of the variation in m at different true strains in the homogenous deformation part of the stress–strain curves are shown in Fig. 6. This figure shows that there is considerable difference between the values of m for the spheroidized, the quench-tempered, and the normalized specimens. It can be seen that there is a direct relation between the strain rate and m for the normalized and the spheroidized specimens and an inverse relation for the quench-tempered specimens. The reason is attributed to the different microstructures and mechanical properties of the spheroidized and the normalized specimens from those of the quench-tempered specimens. It should be noticed that generally m increases as the yield strength decreases. Materials with low yield strengths, such as the spheroidized and normalized steels, possess a higher

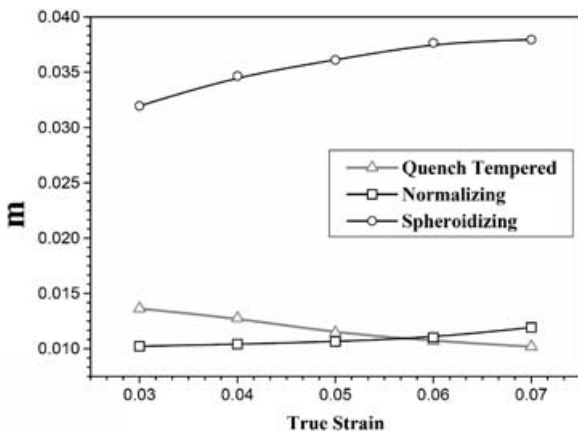


Fig. 6 Variation in the strain rate sensitivity parameter versus true strain as a function of heat treatment for AISI 4140 steel

m value than high-yield-strength materials such as the quench-tempered steels.

Figure 7 compares the engineering stress–engineering strain curves of specimens 10 to 12 with specimen 7. All samples have been tested at the same strain rate condition, i.e. 0.167 min^{-1} . The mechanical properties of the specimens, which are obtained from the engineering stress–engineering strain curves, are summarized in Table 5. Figure 8 shows the true stress–true strain curves of quench-tempered specimens. To investigate the influence of quench-tempering condition on stress–strain curve parameters, i.e. n , K , and m , the homogenous deformation parts of the true stress–true strain curves were drawn on a log–log scale (Fig. 9). The summary of calculated parameters is shown in Table 6.

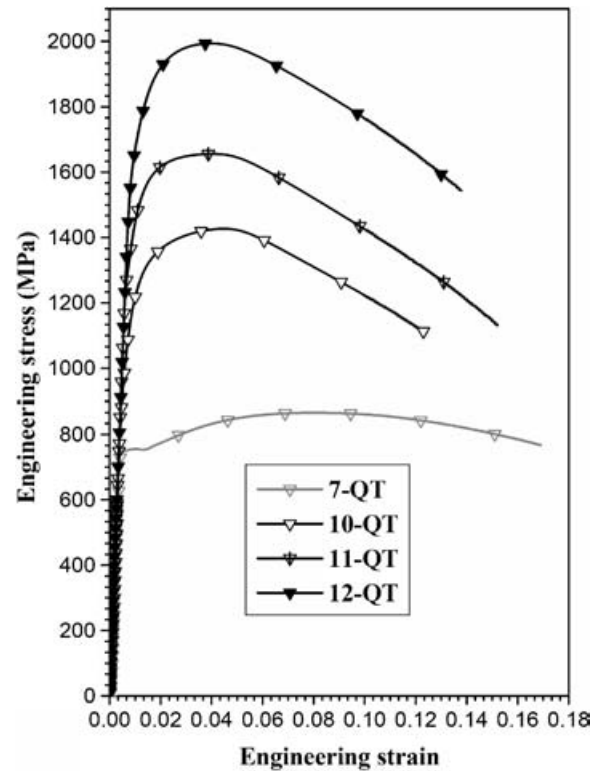


Fig. 7 Engineering stress–engineering strain curves of quench-tempered specimens at a strain rate of 0.167 min^{-1}

Table 5 Mechanical properties of quench-tempered specimens with a strain rate of 0.167 min^{-1}

Specimen	Strain rate (min^{-1})	Yield stress (MPa)	Tensile stress (MPa)
7	0.167	749.07	866.33
10	0.167	1356.32	1471.62
11	0.167	1407.11	1665.67
12	0.167	1660.61	1998.23

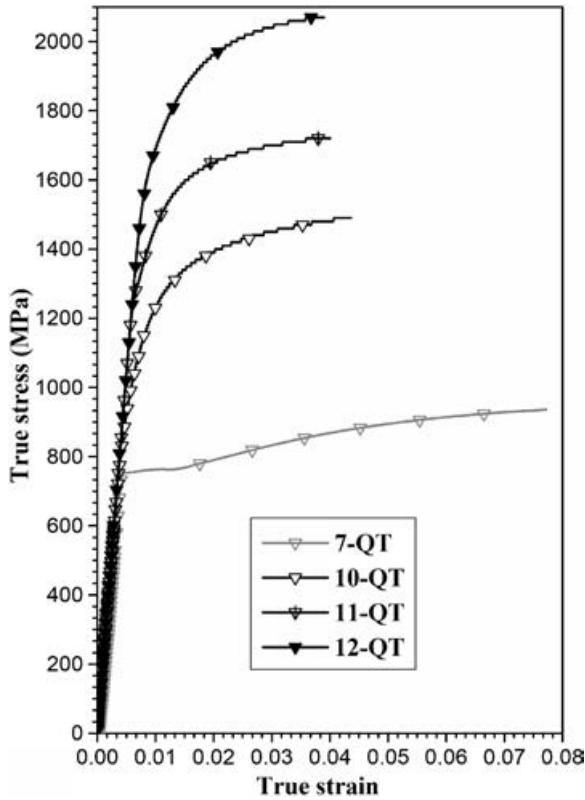


Fig. 8 True stress–true strain curves of quench-tempered specimens at a strain rate of 1.667 min^{-1}

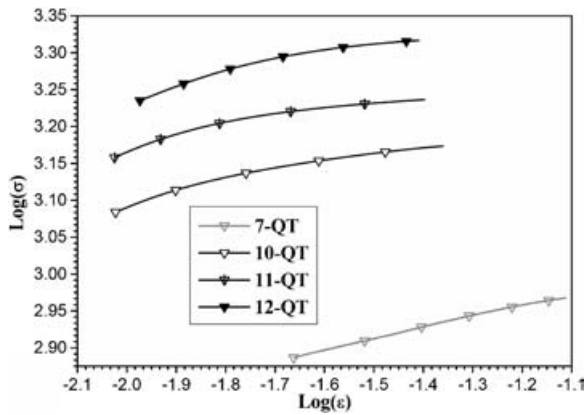


Fig. 9 True stress–true strain curves of quench-tempered specimens on a logarithmic scale with a strain rate of 0.167 min^{-1}

Table 6 Mechanical characteristics of quench-tempered specimens with a strain rate of 0.167 min^{-1}

Specimen	<i>n</i>	<i>K</i> (MPa)
7	0.1499	1372.8
10	0.1278	1958.4
11	0.1191	2590.6
12	0.1441	3396.3

To clarify the influence of the quench-tempered microstructure on the stress–strain curves and their parameters, metallography of the tensile specimens was performed. The scanning electron micrographs in Fig. 10 show the microstructures in the centre of

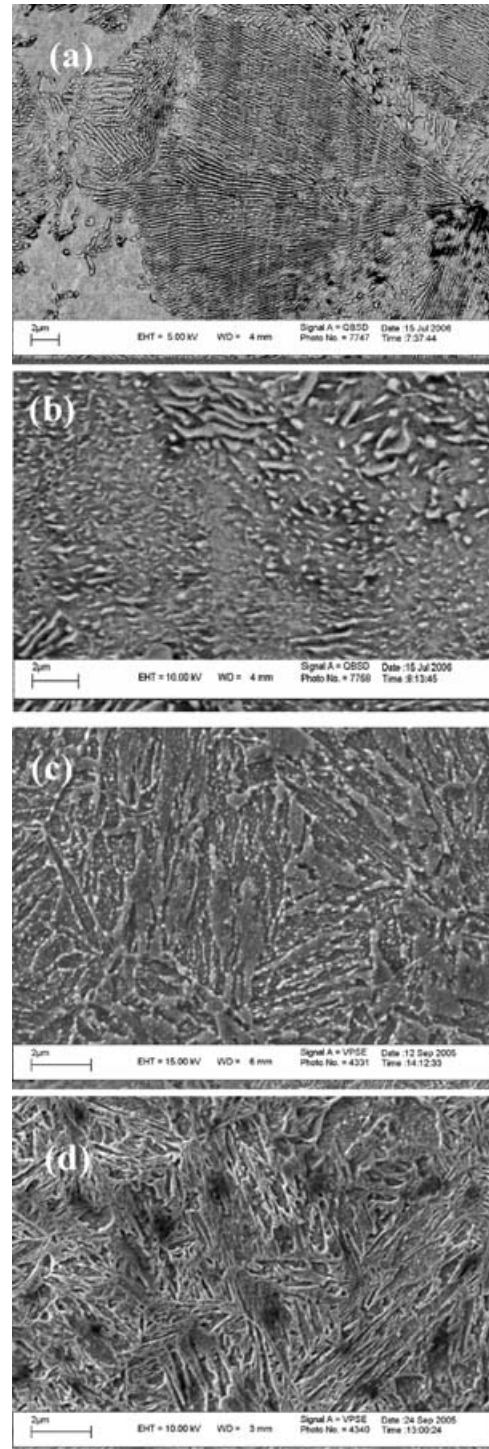


Fig. 10 Scanning electron micrographs of specimens: (a) normalized specimen; (b) spheroidized specimen; (c) quench-single-tempered specimen; (d) quench-double-tempered specimen

the specimens. Carbide growth can be observed as both the time and the temperature of the tempering treatment increase. The present authors believe that the true reason for the appearance of the yielding phenomenon can be attributed to the carbide size and its distribution inside the matrix. Since the carbon content in the ferrite matrix in the spheroidized microstructure is much lower than in the other microstructures, thus the Lüders strain can be small [31, 32].

4 CONCLUSION

In this paper the dependence of the mechanical characteristics of AISI 4140 steel on both the strain rate and the microstructure is investigated. The conclusions are summarized as follows.

1. The quench-tempered microstructure has lower n and K than both the spheroidized and the normalized structures and the responses of the quench-tempered and the normalized structures are the same as the strain rate increases.
2. The strain rate sensitivity of the spheroidized structure is about three times higher those of the other structures.
3. At the same strain rate, AISI 4140 steel has different yield point phenomenon behaviours.
4. The appearance of the yield point phenomenon can be attributed to the growth of carbides and the ferrite matrix content.
5. The Lüders strain width depends on the microstructure. For instance the Lüders strain can be eliminated in the quench-tempered structure by decreasing the tempering temperature.

REFERENCES

- 1 Grange, R. Strengthening by austenite grain refinement. *Trans. Am. Soc. Metals*, 1966, **59**, 26–29.
- 2 Mahajan, S., Venkataraman, G., and Mallik, A. K. Grain refinement of steel cyclic rapid heating. *Metallography*, 1973, **6**, 337–345.
- 3 Krauss, G. *Steels, heat treatment and processing principles*, 1990 (ASM International, Materials Park, Ohio).
- 4 Petch, N. J. The cleavage strength of polycrystals. *J. Iron Steel Inst., London*, 1953, **174**, 25–28.
- 5 Low, J. R. *Relation of properties to microstructure*, 1954, pp. 163–168 (ASM International, Materials Park, Ohio).
- 6 Smoljan, B. An analysis of combined cyclic heat treatment performance. *J. Mater. Processing Technol.*, 2004, **155–156**, 1704–1707.
- 7 Fedyukin, V. *Thermal cycling treatment of steels and cast irons* (in Russian), 1984 (Leningrad State University, Leningrad).
- 8 Konopleva, E. Thermal cycling treatment of low-carbon steel with hardening from intercritical temperature range. *Metal Sci. Heat Treatment Metals*, 1989, **8**, 617–621.
- 9 Smoljan, B. Contribution to investigation of the thermal cycling treatment of steel. In *Proceedings of the Ninth International Congress on Heat treatment and surface engineering*, Nice, France, 1994, pp. 49–58 (PYC Edition).
- 10 Gaponov, Y., Marchenko, V. G., Shtein, Y. A., and D'yachenko, S. S. Influence of thermal cycling treatment to the critical points of steel. *Metal Sci. Heat Treatment Metals*, 1988, **7**, 493–501.
- 11 Radovic, M., Lara-Curzio, E., and Riester, L. Comparison of different experimental techniques for determination of elastic properties of solids. *Mater. Sci. Engng: A*, 2004, **368**, 56–70.
- 12 Davis, J. R. (Ed.) *Metals handbook*, 1990 (ASM International, Materials Park, Ohio).
- 13 Armstrong, P. E. and Bunshan, R. F. (Eds) *Measurement of mechanical properties, techniques of metals research*, Vol. V, Part 2, 1971, pp. 103–107 (John Wiley, New York).
- 14 Lenard, J. G., Pietrzyk, M., and Cser, L. *Mathematical and physical simulation of the properties of hot rolled products*, 1999, pp. 73–75 (Elsevier, Amsterdam).
- 15 Misaka, Y. and Yoshimoto, T. Formulation of mean resistance of deformation of plain carbon steel at elevated temperature. *J. Jap. Soc. Technol. Plast.*, 1967–1968, **8**, 414–422.
- 16 Siciliano, F. and Jonas, J. J. Mathematical modeling of hot strip rolling of microalloyed Nb, multiply-alloyed Cr–Mo, and plain C–Mn steels. *Metall. Mater. Trans. A*, 2000, **31**, 511–530.
- 17 Shida, S. Empirical formula of flow stress of carbon steels resistance to deformation of carbon steels at elevated temperature. 2nd Report (in Japanese). *J. Jap. Soc. Technol. Plast.*, 1969, **10**, 610–617.
- 18 Sarioğlu, F. The effect of tempering on susceptibility to stress corrosion cracking of AISI 4140 steel in 33% sodium hydroxide at 80 °C. *Mater. Sci. Engng: A*, 2001, **315**, 98–102.
- 19 Holzapfel, H., Schulze, V., Vöhringer, O., and Macherauch, E. Residual stress relaxation in an AISI 4140 steel due to quasistatic and cyclic loading at higher temperatures. *Mater. Sci. Engng: A*, 1998, **248**, 9–18.
- 20 Holzapfel, H. *Das Abbaueverhalten kugelstrahlbedingter Eigenspannungen bei 42CrMo4 in Verschiedenen Wärmebehandlungszuständen*. Dr-Ing. Dissertation, Universität Karlsruhe (Technische Hochschule), 1994.
- 21 Holzapfel, H., Schulze, V., Vöhringer, O., and Macherauch, E. Relaxation behaviour of shot peening induced residual stresses in AISI 4140 due to quasistatic uniaxial loading at elevated temperatures. In *Proceedings of the Sixth Conference on*

- Shot peening* (Ed. J. Champaigne), San Francisco, California, USA, 1996, pp. 385–396 (International Scientific Committee for Shot Peening, Tokyo).
- 22 **Ebenau, A.** *Das Verhalten von kugelgestrahltem 42 CrMo 4 im normalisierten und vergüteten Zustand unter einachsiger homogener und inhomogener Wechselbeanspruchung*. Dr-Ing. Dissertation, Universität Karlsruhe (Technische Hochschule), 1989.
- 23 **Eifler, D.** *Inhomogene Deformationserscheinungen bei Schwingbeanspruchung eines unterschiedlich wärmebehandelten Stahles des Typs 42CrMo4*, Dr-Ing. Dissertation, Universität Karlsruhe (Technische Hochschule), 1981.
- 24 **Hall, A. M.** *Introduction to today's ultrahigh-strength structural steels*, ASTM STP 498, 1971 (ASTM International, Philadelphia, Pennsylvania).
- 25 **Unterweiser, P. M.** *Heat treater's guide*, 1995, pp. 120–180 (American Society for Metals).
- 26 **Thelning, K. E.** *Steel and its heat treatment*, 1975, pp. 584–590 (Butterworth, London).
- 27 **Jost, W.** *Diffusion in solids, liquids and gases*, 1952 (Academic Press, New York).
- 28 **Datsko, J.** *Material properties and manufacturing processes*, 1966, pp. 18–20 (John Wiley, New York).
- 29 **Ludwigson, D. C.** Modified stress-strain relation for FCC metals and alloys. *Metall. Trans.*, 1971, **2**, 2825–2828.
- 30 **Morrison, W. B.** The effect of microstructure on mechanical properties of low carbon steel. *Trans. Am. Soc. Metals*, 1966, **59**, 824–829.
- 31 **Sowerby, R.** and **Duncan, D. L.** Failure in sheet metal in biaxial tension. *Int. J. Mech. Sci.*, **13**, 217–229.
- 32 **Hall, E. O.** *Yield point phenomena in metals and alloys*, 1970 (Plenum, New York).
- 33 **Dhar, A., Clapham, L., and Atherton, D. L.** Influence of Lüders bands on magnetic Bauhauser noise and magnetic flux leakage signals. *J. Mater. Sci.*, 2002, **37**, 2441–2446.